Stockholm University

Atmospheric and oceanic circulation from a thermodynamic perspective

Aitor Aldama Campino

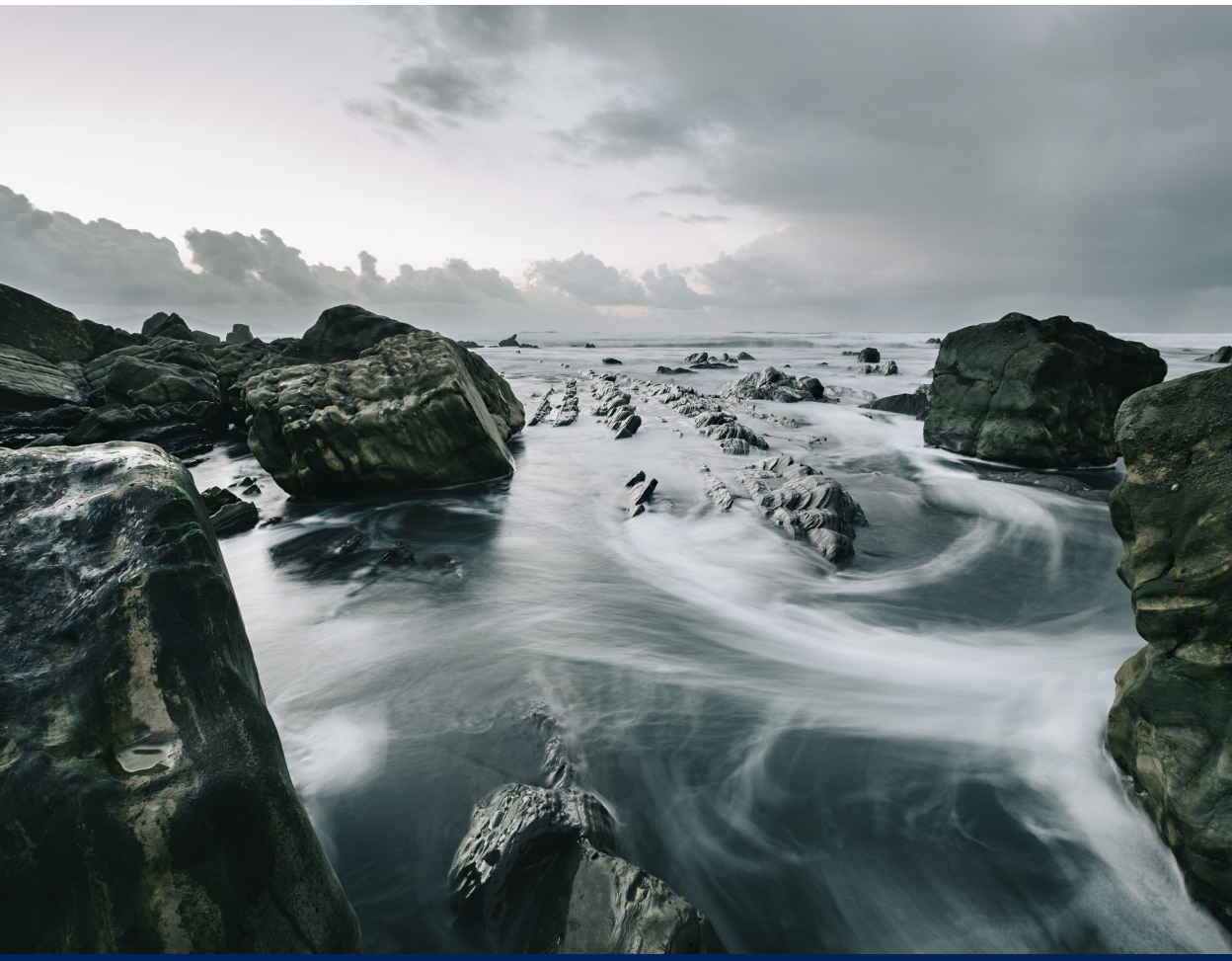

Doctoral Thesis in Atmospheric Sciences and Oceanography at Stockholm University, Sweden 2019

Atmospheric and oceanic circulation from a thermodynamic perspective

Aitor Aldama Campino

Academic dissertation for the Degree of Doctor of Philosophy in Atmospheric Sciences and Oceanography at Stockholm University to be publicly defended on Thursday 24 October 2019 at 10.00 in De Geersalen, Svante Arrhenius väg 14.

Abstract

The climate system is continuously transporting and exchanging heat, freshwater, carbon and other tracers in different spatio-temporal scales. Therefore, analysing the system from a thermodynamic or biogeochemical framework is highly convenient. In this thesis the interaction between the ocean and the atmospheric circulation is analysed using thermodynamical and biogeochemical coordinates. Due to the dimensionality of the climate system stream functions are used to reduce this complexity and facilitate the understanding of the different processes that take place. The first half of this thesis, focuses on the interaction between the atmospheric and the ocean circulation from a thermodynamic perspective. We introduce the hydrothermohaline stream function which combines the atmospheric circulation in humidity-potential temperature (*hydrothermal*) space and the ocean circulation in salinity-temperature coordinates (*thermohaline*). A scale factor of 7.1 is proposed to link humidity and salinity coordinates. Future scenarios are showing an increase of humidity in the atmosphere due to the increase of temperatures which results in a widening of the hydrothermal stream function along the humidity coordinate. In a similar way, the ocean circulation in the thermohaline space expands along the salinity coordinate. The link between salinity and humidity changes is strongest at net evaporation regions where the gain of water vapour in the atmosphere results in a salinification in the ocean. In addition, the ocean circulation in latitude-carbon space is investigated. By doing so, we are able to distinguish the roles of different water masses and circulation pathways for ocean carbon. We find that the surface waters in the subtropical gyres are the main drivers of the meridional carbon transport in the ocean. By separating the carbon in its different constituents we show that the carbon transported by the majority of the water masses is a result of the solubility pump. The contribution of the biological pump is predominant in the deep Pacific Ocean. The effects of the Mediterranean Overflow Waters on the North Atlantic are discussed in the final part of the thesis.

Keywords: *Atmospheric circulation, Ocean circulation, Stream functions.*

Stockholm 2019
http://urn.kb.se/resolve?urn=urn:nbn:se:su:diva-172842

ISBN 978-91-7797-827-5
ISBN 978-91-7797-828-2

Department of Meteorology

Stockholm University, 106 91 Stockholm

ATMOSPHERIC AND OCEANIC CIRCULATION FROM A THERMODYNAMIC PERSPECTIVE

Aitor Aldama Campino

Stockholm
University

Atmospheric and oceanic circulation from a thermodynamic perspective

Aitor Aldama Campino

ISBN print 978-91-7797-827-5
ISBN PDF 978-91-7797-828-2

Cover image: wave breaking in Meñakoz Cove, Basque Country. Photo by Jon del Rivero.

Printed in Sweden by Universitetsservice US-AB, Stockholm 2019

To my parents Bego and Josu

Abstract

The climate system is continuously transporting and exchanging heat, freshwater, carbon and other tracers in different spatio-temporal scales. Therefore, analysing the system from a thermodynamic or biogeochemical framework is highly convenient. In this thesis the interaction between the ocean and the atmospheric circulation is analysed using thermodynamical and biogeochemical coordinates. Due to the dimensionality of the climate system, stream functions are used to reduce this complexity and facilitate the understanding of the different processes that take place.

The first half of this thesis, focuses on the interaction between the atmospheric and the ocean circulation from a thermodynamic perspective. We introduce the hydrothermohaline stream function which combines the atmospheric circulation in humidity-potential temperature (*hydrothermal*) space and the ocean circulation in salinity-temperature coordinates (*thermohaline*). A scale factor of 7.1 is proposed to link humidity and salinity coordinates. Future scenarios are showing an increase of humidity in the atmosphere due to the increase of temperatures which results in a widening of the hydrothermal stream function along the humidity coordinate. In a similar way, the ocean circulation in the thermohaline space expands along the salinity coordinate. The link between salinity and humidity changes is strongest at net evaporation regions where the gain of water vapour in the atmosphere results in a salinification in the ocean.

In addition, the ocean circulation in latitude-carbon space is investigated. By doing so, we are able to distinguish the roles of different water masses and circulation pathways for ocean carbon. We find that the surface waters in the subtropical gyres are the main drivers of the meridional carbon transport in the ocean. By separating the carbon in its different constituents we show that the carbon transported by the majority of the water masses is a result of the solubility pump. The contribution of the biological pump is predominant in the deep Pacific Ocean. The effects of the Mediterranean Overflow Waters on the North Atlantic are discussed in the final part of the thesis.

Sammanfattning

Klimatsystemet transporterar och utbyter kontinuerligt värme, sötvatten, kol och andra markörer i olika skalor för tid och rum. Därför är det mycket praktiskt att analysera systemet med ett termodynamiskt eller biogeokemiskt synsätt. I denna avhandling analyseras interaktionen mellan havets och atmosfärens cirkulation genom nyttjandet av termodynamiska och biogeokemiska koordinater. På grund av klimatsystemets dimensionalitet användes strömfunktioner för att minska komplexiteten och underlätta förståelsen för de olika processerna.

Den första halvan av denna avhandling fokuserar på interaktionen mellan atmosfärens och havets cirkulation ur ett termodynamiskt perspektiv. Vi introducerar den hydrotermohalina strömfunktionen som kombinerar den atmosfäriska cirkulationen i koordinater av luftfuktighet och potentiell temperatur (*hydrotermisk*) med havets cirkulation i koordinater av salinitet och temperatur (*termohalin*). En skalfaktor på 7,1 föreslås för att sammankoppla luftfuktighet och salinitetskoordinater. Framtida scenarier visar en ökning av luftfuktigheten i atmosfären på grund av temperaturökningar som resulterar i en utvidgning av den hydrotermiska strömfunktionen längs fuktkoordinaten. På liknande sätt expanderar havets cirkulation i det termohalina rummet längs salinitetskoordinaten. Kopplingen mellan förändringar i salinitet och luftfuktighet är starkast vid regioner med nettoavdunstning, där avdunstningen av vattenånga i atmosfären resulterar i en försaltning av havet.

Dessutom undersöks havets cirkulation i latitud-kolrummet. Därmed kunde vi skilja på olika vattenmassor och cirkulationsvägar för kolet i havet. Vi finner att ytvattnet i de subtropiska virvlarna är den viktigaste drivkraften för den meridionala koltransporten i havet. Genom att dela upp kolet i dess olika beståndsdelar visar vi att kolet som transporteras av majoriteten av vattenmassorna är ett resultat av löslighetspumpen. Den biologiska pumpens bidrag är dominerande i det djupa Stilla havet. Effekterna av Medelhavets överflödesvatten på Nordatlanten diskuteras i den sista delen av avhandlingen.

Laburpena / Resumen

Lurreko klima sistemak etengabe garraiatzen eta trukatzen ditu beroa, ura, karbonoa eta bestelako adierazleak espazio-denbora eskala desberdinetan. Hortaz, sistema ikuspuntu termodinamiko edo biokimiko batetik aztertzea oso egokia da. Tesi honetan ozeanoen eta atmosferaren zirkulazioen arteko elkarrekintzak koordenatu termodinamikoak eta biogeokimikoak erabiliz aztertu egin dira. Klima-sistemaren dimentsionaltasuna dela eta, korronte funtzioak erabili dira konplexutasun hori murrizteko eta bertan jazotzen diren prozesu desberdinen ulermena errazteko.

Tesi honen lehenengo zatia, atmosferaren eta ozeanoaren zirkulazioen arteko elkarrekintzan oinarritzen da ikuspegi termodinamikotik. Hortarako, hidrotermohalina korronte funtzioa aurkeztu dugu. Funtzio honek atmosferaren zirkulazio *hidrotermala* (hezetasun eta temperatura potentzialan oinarrituta) eta ozeanoaren zirkulazio *termohalina* (gazitasun eta tenperaturan oinarrituta) uztartzen ditu. Hezetasun eta gazitasun koordenatuak lotzeko 7,1 eskala faktorea proposatzen dugu. Etorkizuneko iragarpenetan atmosferako hezetasuna areagotzen ari da tenperaturen igoera dela eta. Ondorioz, korronte funtzio hidrotermala hezetasun koordenatuan hedatuko da. Modu berdinean, ozeanoaren zirkulazioa espazio ter-

El sistema climático está continuamente transportando e intercambiando calor, agua dulce, carbono y otros trazadores en diferentes escalas espacio-temporales. Por lo tanto, analizar el sistema desde un marco termodinámico o biogeoquímico es muy conveniente. En esta tesis, la interacción entre las circulaciones oceánica y atmosférica es analizada utilizando coordenadas termodinámicas y biogeoquímicas. Debido a la gran dimensionalidad del sistema climático, las funciones de corriente son utilizadas para reducir esta complejidad y facilitar la comprensión de los diferentes procesos dentro del sistema.

La primera mitad de esta tesis se centra en la interacción entre la circulación atmosférica y oceánica desde una perspectiva termodinámica. La función de corriente hidrotermohalina es presentada; la cual combina la circulación atmosférica, definida en coordenadas de humedad y temperatura potencial (*hidrotérmica*), y la circulación oceánica en coordenadas de salinidad y temperatura (*termohalina*). Un factor de escala de 7.1 vinculando las coordenadas de humedad y salinidad es propuesto. Las proyecciones a futuro muestran un aumento de la humedad en la atmósfera debido al aumento de las temperaturas que resulta en un ensanchamiento de la función de cor-

mohalinoan gazitasun-koordenatuan zehar hedatuko da. Gazitasun eta hezetasun aldaketen arteko lotura tinkoagoa da lurrunketa netoa gertatzen den eskualdeetan. Atmosferak ur lurruna irabazten duen bitartean ozeanoaren gainazala gazitzen da.

Bestalde, ozeanoen zirkulazioa latitude-karbono eremuan aztertu egin dugu. Modu honetan, ur masa desberdinen eta karbonoaren ibilbide desberdinen rolak bereizteko gai gara. Bira subtropikal handien gainazaleko urak ipar-hego norabideko karbono garraioaren eragile nagusiak direla aurkitu dugu. Karbonoa bere osagai desberdinetan bereiziz, ur masa gehienek garraiatutako karbonoa ponpa fisikoaren emaitza dela aurkitu dugu. Ponpa biologikoaren ekarpena nagusiki Ozeano Bareko sakonean jazotzen da. Mediterraneo itsasoko uren eraginak Ipar Atlantikoan tesiaren azken zatian eztabaidatu egin dira.

riente hidrotérmica a lo largo de la coordenada de humedad. De manera similar, la circulación oceánica en el espacio termohalino se expande a lo largo de la coordenada de salinidad. El vínculo entre los cambios de salinidad y humedad es más fuerte en las regiones de evaporación neta donde la ganancia de vapor de agua en la atmósfera resulta en una salinificación de la superficie del océano.

Además, la circulación oceánica es investigada usando las coordenadas de latitud y carbono. De este modo podemos distinguir el rol que juegan las diferentes masas de agua y las vías de circulación del carbono en el océano. Las aguas superficiales localizadas en los giros subtropicales son las principales impulsoras del transporte meridional de carbono en el océano según nuestros resultados. Al separar el carbono en sus diferentes componentes mostramos que el carbono transportado por la mayoría de las masas de agua en el océano es el resultado de la bomba de solubilidad. La contribución de la bomba biológica es predominante en las profundidades del océano Pacífico. Los efectos de las aguas de desbordamiento del mar Mediterráneo en el Atlántico Norte son presentados en la parte final de la tesis.

List of Papers

The following papers, referred to in the text by their Roman numerals, are included in this thesis.

Paper I: K. Döös, J. Kjellsson, J.D. Zika, F. Laliberté, L. Brodeau, and **A. Aldama Campino** (2017).
The Coupled Ocean-Atmosphere Hydrothermohaline Circulation
Journal of Climate, **30**, 631-647. ©American Meteorogical Society. Used with permission.
DOI: `http://dx.doi.org/10.1175/JCLI-D-15-0759.1`

Paper II: **A. Aldama Campino**, and K. Döös.
The effects of global warming on the coupled Ocean-Atmosphere Hydrothermohaline circulation.
Submitted to Geophysical Research Letters, under review

Paper III: **A. Aldama Campino**, F. Fransner, M. Ödalen, S. Groeskamp, A. Yool, K. Döös, J. Nycander.
Meridional ocean carbon transport.
Submitted to Global Biogeochemical Cycles, under review

Paper IV: **A. Aldama Campino**, and K. Döös.
The Mediterranean Overflow Water in the North Atlantic and its multidecadal variability.
Accepted in Tellus A

Reprints were made with permission from the publishers.

Author's contribution

Kristofer Döös is the main author in **Paper I**. I contributed to the method and the mathematical computation of this paper.

For **Paper II**, the idea came from discussions between Kristofer Döös and me. I contributed to the development of the scientific ideas and questions in the paper. I collected and analysed the data and produced the figures. I wrote the manuscript with inputs from Kristofer Döös. After submission, I also performed the required revisions.

The first idea of **Paper III** was based on discussions with Kristofer Döös, Sjoerd Groeskamp and me during the workshop on "Thermodynamic analysis for atmospheric and oceanic flows" that took place in Abu-Dhabi (UAE) in February 2016. Filippa Fransner and Malin Ödalen contributed significantly to the scientific discussion of this work. The model output data was provided by Andrew Yool. I adapted the analysis model code for the experimental design, analysed the data and produced the figures. I wrote the majority of the manuscript except sections 2.1 written by Malin Ödalen, and sections 2.3 written by Andrew Yool and Filippa Fransner.

Paper IV was based on discussions with Kristofer Döös and me during the workshop on the Atlantic Meridional Overturning Circulation that took place in Stockholm (Sweden) in September 2015. I performed all the data analysis, wrote the manuscript and made revisions suggested by the co-authors. After submission, I also performed the required revisions.

Abbreviations

AABW	Antarctic Bottom Water
AMOC	Atlantic Meridional Overturning Circulation
C-C	Clausius-Clapeyron relationship
DSE	Dry Static Energy
LH	Latent Heat
LIW	Levantine Intermediate Water
MOW	Mediterranean Overflow Water
NADW	North Atlantic Deep Water
NAO	North Atlantic Oscillation
SSS	Sea Surface Salinity
SST	Sea Surface Temperature
WMDW	Western Mediterranean Deep Water

Contents

1. Introduction

It all started with a simple experiment in 1751 somewhere in the subtropical Atlantic Ocean. During one of the multiple trans-Atlantic crossings Captain Henry Ellis[1] took some temperature measurements of the ocean. For that purpose, he used an ingenious invention that consisted of a bucket with flaps that could trap the water at different depths. In the beginning, the measurements showed some tendency; the deeper he dipped the bucket, the colder the water temperature was. However, at depths below 1200 m the water temperature barely changed. This was the first time that deep ocean waters were measured. While puzzled and unable to explain the observations he wrote that *"this experiment [...] became in the interim very useful to us. By its means we supplied our cold bath, and cooled our wines or water at pleasure; which is vastly agreeable to us in this burning climate"* (Ellis & Hales, 1751).

The findings of Henry Ellis were rediscovered by Benjamin Thomson[2] in 1797. Thomson, whose scientific work was centred on the nature of heat, discarded the established idea that the deep ocean waters were slowly warming up from the surface. If that hypothesis would have been true, it could not have explained the cold waters measured by Ellis. Instead, Thomson came to the conclusion that the deep ocean water should have come from the polar regions. *"What has been called the Gulf Stream in the Atlantic Ocean is no other than one of these currents that at the surface which moves from the equator to the north pole [...] ; the lower current may be considered as proved by the cold which has been found to exist at great depths in warm latitudes [...] which of course must have been brought from colder latitudes"* (Thomson, 1797). Without the help of satellites and modern *in-situ* observational tools, Thomson described, using a simplified schematic, the complex ocean circulation.

Trying to understand such a complex system was and still is a challenge. How could we describe in a simple way a system that requires three spatial dimensions in addition to time, which covers from microscopic to planetary scales and time scales from few seconds to millennia? Besides, the lack of enough observations that cover all the scales makes it further complicated. But even with the introduction of satellites in 1970s, which significantly improved the observations of the atmosphere, the problem remained particularly for the ocean.

[1] Captain Henry Ellis (1721-1806): was an explorer and colonial governor of Georgia and Nova Scotia. He worked as slave trader between 1750-1755.

[2] Benjamin Thomson, Count Rumford (1753-1814): was an anglo-american physicist and inventor.

Satellites have become useful for providing a broad picture of the surface of the ocean. However, even with all the actual observational tools (*e.g.* satellites, ship tracks, buoys, autonomous vehicles) we are unable to get a complete 3-D picture of the ocean. This is a well known and fundamental problem in oceanography where the deep ocean remains being a region with many open questions.

Numerical models have become useful to fill the lack of observations. Nevertheless, the amount of data and information is still large. All that information needs to be optimised in such a way that facilitates the understanding of the dynamics, the different processes, *etc.* that take place in the system. This optimisation and visualisation techniques cover different methods: from simple cross sections, or temperature-salinity diagrams; to more advanced statistical tools like Empirical Orthogonal Functions (Hannachi *et al.*, 2007), Principal Component Analysis (Pauthenet *et al.*, 2019) or stream functions.

The main aim of this thesis is to contribute to the understanding of atmospheric and ocean circulation in a thermodynamic and biogeochemical framework. The main approach has been done using stream functions in pure thermodynamic coordinates (Paper I and Paper II), or combining geographical and tracer coordinates (Paper III), to pure geographical coordinates (Paper IV).

- In Paper I we discuss how to couple the atmospheric and the ocean circulation using stream functions.
- In Paper II the results of Paper I are revisited. We analyse how the global warming affects and modifies the thermodynamic stream functions.
- The use of a biogeochemical tracer as coordinate for a stream function is introduced in Paper III.
- The impact of the overflow waters from the Mediterranean Sea on the Atlantic circulation is discussed in Paper IV.

This introductory part of the thesis is organised as follows: in Chapter 2 a short introduction to the climate system is presented. The numerical models used in this thesis are described in Chapter 3. A mathematical description on how stream functions and the associated transports are computed is presented in Chapter 4. In Chapter 5, some examples of the most relevant stream functions are introduced. A brief description of the Mediterranean Sea and its influence on the Atlantic Ocean is presented in Chapter 6. Finally, the final remarks of this thesis and the future outlook are given in Chapter 7.

2. Climate System

2.1 Atmospheric circulation

The atmospheric circulation has also its particular story. One of the key questions in the past was to understand the way air parcels are transported from the tropics to high latitudes. The first attempt was performed by Edmond Halley[1] in 1686. His idea was simple: the warm air in the tropics rises, eventually hits a ceiling of sorts (the tropopause) and spreads poleward. At high latitudes the air mass sinks back to the surface, and the circuit is closed by surface winds toward the tropics (Halley, 1686). George Hadley[2] supported Halley's idea that the temperature difference between the low and the high latitudes was responsible for the atmospheric circulation. However, Hadley corrected Halley's model by introducing Earth's rotation. This way Hadley was able to explain the trade winds in the tropical region compared to the pure meridional winds formulated by Halley (Hadley, 1735).

Hadley's model, based on a single hemispheric cell (see Figure 2.1), was unable to explain the poleward winds on average at mid-latitudes (Ferrel, 1856). In the mid 1850-s, two independent models were introduced to correct Hadley's model. Thomson's[3] model suggested a two cell system adding a "*thin stratum*" below the large cell from Hadley's model. This secondary circulation cell was located at the mid-latitudes and was responsible for the poleward winds in the area (Thomson, 1857). Two years later, Ferrel's[4] three-cell model was introduced. Ferrel's model split the large cell from Hadley's model in two independent thermally driven cells. The model introduced a third cell at mid-latitudes similar to the one introduced by Thomson but much larger and deeper (see Figure 2.1). Ferrel proposed that an imbalance of the Earth's rotation and the air pressure gradient was responsible for this cell (Ferrel, 1859).

Although the meridional flow of air is an important key in the atmospheric circulation, zonal flows also play a crucial role. One of the most major east-west flow is the Walker circulation in the tropical region. The most well known cell in this circulation is the Walker Cell (Peixoto & Oort, 1992). This cell was

[1] Edmond Halley (1656-1742): english astronomer, physicist, meteorologist and mathematician. Known for descovering the periodicity of the comet named after him.

[2] George Hadley (1685-1768): english lawyer and meteorologist.

[3] James Thomson (1822-1892): Irish engineer and physicist. His achivements were shadowed by those done by his younger brother William Thomson (Lord Kelvin).

[4] William Ferrel (1817-1891): American meteorologist and astronomer.

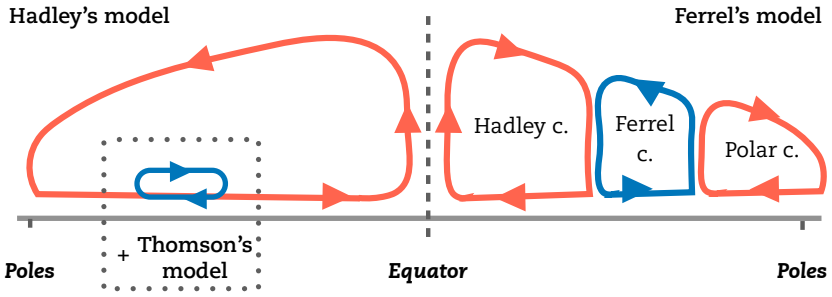

Figure 2.1: Sketch of the meridional motion of air masses from the tropics to the poles. The Hadley model (left hand side) is described by a large hemispheric cell from the tropics to the poles. Thomson's model is similar to Hadley's but with a thin and shallow secondary circulation in the mid-latitudes. The Ferrel model (right hand side) is represented by three independent cells per hemisphere.

discovered by Gilbert Walker[1] in 1924. Walker was very interested in the study of the predictability of the Asian Monsoon in order to prevent future famines in the region. These predictability studies were based on correlating the Asian Monsoon to different indices, such as snowfall in the Himalayas (Blandford, 1884), the strength of the trade winds, or even the Nile floods (Eliot, 1895). Walker noticed a strong correlation between the rainfall in the west Pacific ocean and the pressure gradient between the eastern and western tropical Pacific (Walker, 1924). Bjerknes (1969)[2] linked this pressure gradient to a zonal overturning circulation cell (the Walker cell). This cell describes the rising air in the warm pool located in the western Pacific. It is followed by a westerly flow at high altitudes, and sinking of air in the eastern Pacific. Finally, the cell is closed by the surface trade winds. The Walker circulation has an important impact on the sea surface temperature (SST) gradients over the tropical Pacific Ocean. The event known as El Niño is a result of a weakening of the Walker cell and a decrease of the gradient (Neelin *et al.*, 1998, Philander, 1983, Rasmusson & Carpenter, 1982).

2.2 Ocean circulation

The simple sketch described by Thomson (1797) captured the main ingredients of the ocean general circulation: the distribution of density and the boundary conditions (*e.g.* the surface wind-stress, heat and freshwater fluxes). This section will mostly be focused on the density driven circulation.

[1] Gilbert Thomas Walker (1868-1958): British physicist and statistician. He was appointed as head of the meteorological observatories in India without any expertise in the field.

[2] Jakob Bjerknes (1897-1975): American-Norwegian meteorologist. He was son of Vilhelm Bjerknes.

The thermohaline circulation – *thermo* for temperature and *haline* for salinity – is part of the ocean general circulation driven by density gradients of different water masses. The original idea for the thermohaline circulation started for the Atlantic ocean (Richardson, 2008) but slowly evolved incorporating the other basins *e.g.* "the great conveyor belt" introduced by Broecker (1991). The starting point of this circulation can be located in a few narrow locations at high latitudes in the North Atlantic and the Southern Ocean (see Figure 2.2). In these regions the surface waters get denser by releasing heat to the atmosphere and sink to the bottom, filling the abyssal ocean (Kuhlbrodt *et al.*, 2007, Talley, 2013). Due to the equation of continuity, all the water volume that sinks must be compensated by upwelling waters in other regions of the ocean. Surface currents transport these waters into the deep water formation areas closing the circulation.

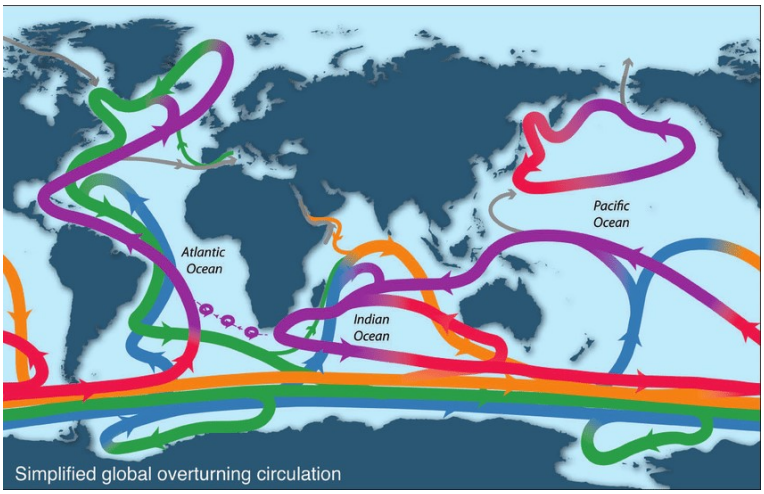

Figure 2.2: Schematic of the global overturning circulation. The different colours represent different water masses. Surface waters are given in red/purple while the deep and bottom waters are given in green/blue. This figure is taken from Talley (2013).

An alternative way of looking at this circulation is using latitude-depth coordinates. In Figure 2.3 a simplified sketch of the two most important cells is presented (Talley, 2013). These cells represent the circulation of the North Atlantic Deep Water (NADW) and the Antartic Bottom Water (AABW). Both water masses are formed by strong heat loss, and salt gain from brine release at high latitudes. While the formation of these two water masses is similar, they have different properties. The AABW is formed around the Antarctica and is the most common water mass found in the bottom of the ocean, while the NADW is formed in the North Atlantic and can be found at deeper layers in the Atlantic ocean. As these water masses move equatorward, mixing with

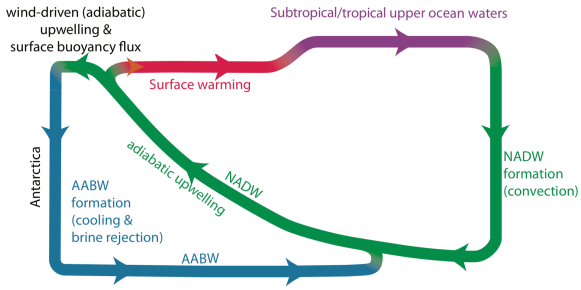

Figure 2.3: Simplified sketch of the NADW and AABW cells. This circulation resembles the overturning circulation in the Atlantic Ocean. Adapted from Talley (2013)

surrounding water masses takes place (Kuhlbrodt *et al.*, 2007). Part of these waters reach the surface through dyapicnal mixing across the ocean stratification. The other part is upwelled due to the strong wind-driven circulation in the Southern Ocean. The NADW cell usually manifests as a meridional overturning circulation known as the Atlantic Meridional Overturning Circulation (AMOC). The AMOC plays an important role transporting large amount of heat from low to high latitudes, and it is largely responsible for the oceanic carbon uptake (Zickfeld *et al.*, 2008).

2.3 Future atmosphere-ocean circulation

Emissions of greenhouse gases (GHG) and aerosols have been shown to have an impact on the global climate system (IPCC, 2013). The observed increase of carbon dioxide, CO_2, concentrations in the atmosphere are for example leading to an increase of surface air temperatures. These changes in the climate system are modifying the global transports of energy and mass in both the atmosphere and the ocean (Caballero & Langen, 2005, Frierson & Hwang, 2012, Hwang & Frierson, 2010, Laliberté *et al.*, 2015, Schneider *et al.*, 2010, Vecchi & Soden, 2007, Vecchi *et al.*, 2006, Weaver *et al.*, 2012).

Using pure thermodynamic arguments, it is possible to estimate the impact of global warming on the atmospheric circulation. It is known that warmer air can hold more water vapour which will lead to an increase of moisture in the atmosphere. This is given by the Clausius-Clapeyron equation (Clapeyron, 1834, Clausius, 1850, Wallace & Hobbs, 2006):

$$\frac{dq_s}{q_s} = \frac{L_v(T)}{R_v T^2} dT = \alpha(T) dT, \tag{2.1}$$

where q_s is the saturation specific humidity, T is the air temperature, L_v is the latent heat for vaporisation, and R_v is the gas constant for water vapour.

Assuming a constant L_v and evaluating equation (2.1) at $T = 273$ K gives a change of saturation specific humidity per temperature of $\alpha(T) = 0.07$ K^{-1}, *i.e.* an increase of humidity of 7% per Kelvin. If the relative humidity remains barely unchanged (Held & Soden, 2000), this would imply that the specific humidity will increase by the same percentage. Future predictions are estimating an increase of precipitation of 1-3% per degree of warming. Precipitation P can be linked, using simple scaling arguments, to the specific humidity q and the upward mass fluxes M which can in turn be linked to the strength of the atmospheric circulation (Held & Soden, 2006):

$$P = Mq. \tag{2.2}$$

Differencing the previous equation, Held & Soden (2006) showed that atmospheric circulation was weakening by $\sim 5\%$ per degree of warming. The difference in the increase of precipitation and the water vapour content in the atmosphere as temperatures increase implies an increase in the residence time of water vapour.

In a global perspective, particularly in zonal averages, future projections show that in regions where evaporation E currently exceeds precipitation P it would do so even more in the future, and *vice versa* (Collins *et al.*, 2013). This is the well known paradigm of "dry gets drier, wet gets wetter". The $E - P$ pattern over oceans controls the freshwater transport between the atmosphere and the ocean. This pattern is strongly linked to the sea surface salinity (SSS) distribution; for instance in subtropical regions where E is dominant the highest SSS values are usually found. Future projections show an analogous of the atmospheric paradigm for SSS, *i.e.* "saline gets more saline, fresh gets fresher" (Durack *et al.*, 2012, Levang & Schmitt, 2015). In Paper I a scale factor between specific humidity q and salinity S is presented. This scale factor is computed assuming a closed freshwater cycle where the freshwater transport in the ocean should balance the one in the atmosphere. Using this argument, the obtained scale factor is approximately:

$$\frac{\Delta q}{\Delta S} \approx 7.1. \tag{2.3}$$

This change of the freshwater forcing will broaden the salinity distribution (Zika *et al.*, 2015). Besides, recent studies have shown that the ocean warming also contributes to sustain the broadening of the salinity distribution due to a stronger stratification near the surface which would prevent a relaxation of the salinity contrasts (Zika *et al.*, 2018). The future salinity distribution will affect the density distribution and hence the thermohaline circulation (Paper II). For example, future projections show warmer and fresher waters in the North Atlantic that would have a significant impact on the deep water formation and on the AMOC (Gent, 2018).

2.4 Carbon decomposition in the ocean

World oceans are an important part of the global carbon cycle. Not only by being the largest reservoir of carbon, but also by exchanging carbon with the atmosphere and land (Ciais *et al.*, 2014). There are two main mechanisms that redistribute carbon from the surface waters to the interior of the ocean: the physical pump and the biological pump (see Figure 2.4).

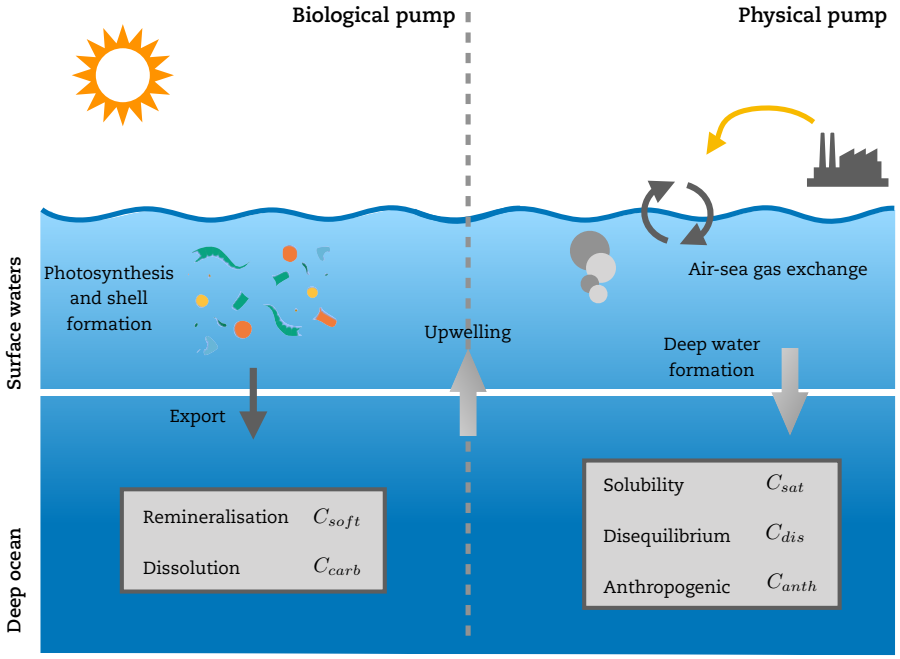

Figure 2.4: Sketch of the physical and biologial pump in the ocean. The physical pump is a result of the gas air-sea exchange. The deep water formation transports the carbon to the deep ocean which is carried back to the surface in the upwelling regions. The biological pump is based on the biological activity at the sea surface. The biological material precipitates to the deep ocean where is remineralised and transformed into inorganic carbon. Adapted from Malin Ödalen.

The physical pump is a result of the dynamics in the ocean. The air-sea gas exchange is more efficient in cold and fresh waters. As the tropical warm waters cool down on their way to the high latitudes, more CO_2 is captured from the atmosphere. The deep water formation at high latitudes transports this carbon to the deep ocean. The reverse effect (release of CO_2) happens in the upwelling region, where cold interior waters are upwelled to the surface. As they warm up, they lose capacity to store carbon and release it to the atmosphere (Volk & Hoffert, 1985, 2013).

The biological pump is also responsible for the transport of carbon to the interior of the ocean. However, the carbon uptake process is different, where biological processes play an important role. The CO_2 is consumed by algae and zooplankton at the ocean surface, where carbon is transformed into living matter (*e.g.* shell formation). When these living forms die, the biological material sinks to the deeper ocean where the action of bacteria releases carbon dioxide. This process is known as remineralisation (Sarmiento & Gruber, 2006, Volk & Hoffert, 1985, 2013).

Carbon in the ocean can be found in both organic and inorganic compounds; however, in this thesis the latter has been studied (Paper III). The dissolved inorganic carbon (DIC) in the ocean can be partitioned into different components (Eggleston & Galbraith, 2018, Ito & Follows, 2005, Ödalen *et al.*, 2018, Williams & Follows, 2011). In this thesis (Paper III) the framework introduced by Lauderdale *et al.* (2013) and Couldrey (2018) has been used:

$$\mathrm{DIC} \equiv C_{tot} = C_{sat} + C_{dis} + C_{anth} + C_{soft} + C_{carb}. \tag{2.4}$$

The first three terms on the right hand side are linked to the physical pump. The saturation carbon, C_{sat}, represents the dissolved carbon that a water mass could contain if it would have enough time to equilibrate with the atmosphere at the sea surface. This component is dependent on the surface waters' temperature, salinity and alkalinity. The contribution of anthropogenic carbon emissions is given by C_{anth}, while the disequilibrium term is given by C_{dis}. The air-sea gas exchange may not be fast enough to equilibrate the surface water masses and as a result they could be over- or under-saturated. Therefore, this term can be either positive or negative. The remaining two terms are part of the biological pump. The remineralisation of biologically fixed carbon is given by C_{soft} which represents the remineralisation of soft tissues, and C_{carb} is linked to the remineralisation of biominerals.

3. Modelling of the climate system

3.1 Atmospheric and ocean circulation models

Numerical models have become essential tools to study the climate system. Models solve most of the governing equations of different processes in each of the sub-systems of the climate system (atmosphere, oceans, sea-ice, ...) and their interactions. As computational resources improve, which help to construct more complex and finer models, we are able to draw a virtual representation of Earth's climate.

Most of the models compute the solutions to the given equations on a three dimensional spatial grid. This means that we are discretising the climate system in small boxes (grid cells). This could become a problem in order to get the "right" solution. As mentioned previously, the climate system ranges from microscopic to planetary scales. Therefore, in order to solve all the different processes we would require a very fine resolution, which would demand huge computational resources. Current resolutions in coupled models are of the order 10-100 kilometres. In order to solve sub-grid processes (processes with length scales smaller than the spatial resolution) we have to parametrise them. When a process is parametrised we are not adding the process itself but its effect. Examples of parametrisation are cloud convection in the atmosphere or geostrophic eddies in the ocean.

For the coupled simulations in Paper I and Paper II the earth system model EC-Earth was used (Hazeleger *et al.*, 2010, 2012). Paper III and Paper IV are based on ocean only simulations from the ocean general circulation NEMO (Madec *et al.*, 2015). The results presented in Paper I, Paper II, and Paper IV are based on a coarse resolution model (around 1° in the ocean and 1.125° in the atmosphere). An intermediate resolution of quarter of a degree in the ocean is used in Paper III. This resolution is eddy permitting but not eddy resolving.

3.2 Biogeochemical models

Biogeochemical cycles are complicated to simulate due to the large amount of tracers and processes that are considered. Simplified versions of these models

only consider a single tracer subjected to simple linear processes. However, the most common models include a variety of tracers (oxygen, zooplankton, etc) and complex non-linear processes. Once coupled to the physical model, the concentration of a tracer C is given by the following equation:

$$\frac{\partial C}{\partial t} = -\mathbf{v} \cdot \nabla C + \nabla_h (K_h \nabla_h) C + \frac{\partial}{\partial z} \left(K_z \frac{\partial C}{\partial z} \right) + F \tag{3.1}$$

where the time evolution of the concentration is controlled (from left to right) by advection, horizontal diffusion, vertical diffusion and biogeochemical fluxes (which include sources and sinks). The carbon uptake is modelled as a function of the uptake of the most limited nutrient set by the Redfield ratio. This ratio describes the molecular proportion of carbon, nitrogen, and phosphorus. This ratio is usually constant in the entire ocean and set to the ratio C:N:P of 106:16:1 (Redfield, 1934).

In Paper III the biogeochemical model MEDUSA (Yool *et al.*, 2013, 2015) is coupled to the physical model NEMO. This intermediate complexity framework contains the elemental cycles of nitrogen, carbon, oxygen, silicon and iron. This model is a nitrogen-based model, with the biological transformations of other elemental cycles related to that of nitrogen by fixed "Redfield" ratios.

4. Stream functions: theory

Stream functions are a well known diagnostic tool used in both atmospheric science and physical oceanography, which help to understand different processes such as volume or mass transports. The idea behind stream functions is a dimensional reduction of the system to a two-dimensional projection. The most traditional stream functions are based on two geographical coordinates, but the stream functions can be built combining a geographical and a tracer coordinate (Döös & Nilsson, 2011, Döös & Webb, 1994, Nycander *et al.*, 2007, Pauluis *et al.*, 2010), or two different tracer coordinates (Döös *et al.*, 2012, Kjellsson *et al.*, 2013, Pauluis & Mrowiec, 2013, Zika *et al.*, 2012).

The units of the stream functions are given in [kg s^{-1}] (which represent a mass transport). For convenience, the results will be presented in mass Sverdrup, 1 Sv$\equiv 10^9$ kg s^{-1}. The Sverdrup is a unit taken from physical oceanography to describe volume transports. However, it can be translated to represent a mass transport by using sea-water density[1].

A mathematical description of the stream functions used in this thesis is presented in the following sections.

4.1 Meridional stream functions

The latitude-depth stream function $\psi(y_0, z_0)$, usually referred to as the meridional overturning stream function is, among the different set of stream functions, the most used and known one. This stream function is computed first by integrating zonally the meridional mass flux to a given depth and then computing a time average:

$$\psi(y_0, z_0) = \frac{1}{\Delta t} \int_{t_0}^{t_0+\Delta t} \int_{-\infty}^{z_0} \int_x F_M^y(x, y_0, z, t) dx dz dt, \tag{4.1}$$

where F_M^y is the meridional mass flux, y_0 and z_0 represent the selected latitude and reference height, respectively. This stream function represents the average total meridional mass transport below a given depth value z_0, at a chosen latitude y_0. If there are no mass sources or sinks, this value also represents the total vertical mass transport north of y_0 at a depth z_0.

[1]The density of sea water is fairly constant $\rho \approx 1000$ kg m^{-3}. Therefore, a volume transport of 1 m^3 s^{-1} is equivalent to 1000 kg s^{-1}.

The meridional overturning circulation can be generalised to any coordinate ξ which could be another geographical coordinate (*e.g.* longitude as in the barotropic stream function $\psi(y,x)$), a thermodynamic coordinate (*e.g.* temperature), or a biochemical tracer (*e.g.* dissolved inorganic carbon). The general equation for a meridional overturning stream function is given by:

$$\psi(y_0,\xi_0) = \frac{1}{\Delta t}\int_{t_0}^{t_0+\Delta t}\int_V \delta[y_0-y]\mu[\xi_0-\xi(\vec{x},t)]F_M^y(\vec{x},t)dV\,dt \tag{4.2}$$

$$= \frac{1}{\Delta t}\int_{t_0}^{t_0+\Delta t}\int_x\int_z \mu[\xi_0-\xi(x,y_0,z,t)]F_M^y(x,y_0,z,t)dz\,dx\,dt \tag{4.3}$$

where $\vec{x}$ is the position vector in geographical coordinates, $\delta[\star]$ is the Dirac delta pseudo-function, and $\mu[\star]$ is the Heaviside step function. By imposing both the Dirac delta function and the step function, the stream function only considers the mass fluxes at y_0 that have a tracer value lower or equal to the chosen ξ_0. Therefore, the general meridional stream function $\psi(y_0,\xi_0)$ represents the mass transport at y_0 of fluid parcels below the selected isoline ξ_0.

There is a set of stream functions where a proper choice of the coordinate ξ transforms the general meridional stream function into an extended version of the meridional overturning circulation. In this case ξ, a non-geographical coordinate, behaves as a pseudo-depth where its values can be related to a depth level. This relation facilitates an estimate of the vertical position in the geographical space besides the mass transport in the $y-\xi$ space. Not all choices of the coordinate ξ are suitable to behave as a pseudo-depth (see Figure 4.1). The suitable coordinate should be well preserved (no internal sources or sinks) and monotonic (no local minimum or maximum value). Tracers such as neutral density γ^n, saturation carbon C_{sat}, or dry static energy (DSE) are good candidates as pseudo-depths.

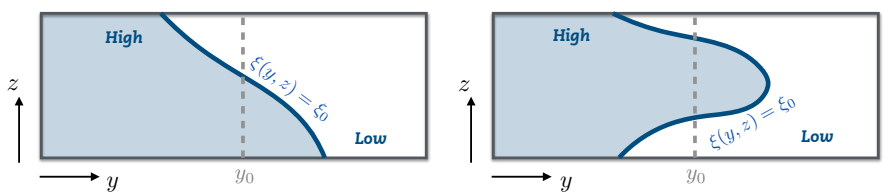

Figure 4.1: Not all tracers can be used as a pseudo-depth. The absence of local minima or maxima of the tracer in the geographical space is a necessary requirement. Left: the tracer ξ can be used as pseudo-depth. Right: the local maximum of ξ prevents this tracer to behave as a pseudo-depth.

4.2 Stream function with two general coordinates $\psi(\lambda_0, \xi_0)$

If both coordinates of the stream function are two different tracers, any geographical information is lost. While this could be a problem to interpret and understand the resulting tracer-tracer stream function, this set of stream functions considers all the mass transports regardless of their directions. The meridional stream function $\psi(y_0, \xi_0)$, for instance, does not capture mass transports in the zonal direction.

The stream function in two general coordinates is given by,

$$\psi(\lambda_0, \xi_0) = \frac{1}{\Delta t} \int_{t_0}^{t_0+\Delta t} \int_V \delta[\lambda_0 - \lambda(\vec{x}, t)] \mu[\xi_0 - \xi(\vec{x}, t)] \frac{D\lambda}{Dt}(\vec{x}, t) \rho dV dt. \quad (4.4)$$

Similar to the meridional stream function, the Dirac delta pseudo-function imposes the isoline value for λ, and the Heaviside step function guarantees mass fluxes below the isoline ξ_0. The third element in the integral $(D\lambda/Dt)$ is the total tendency of the coordinate λ and guarantees that only the mass fluxes perpendicular to the isoline $\lambda = \lambda_0$ are considered in the calculation. Besides, the total tendency also captures possible changes in time of the isolines, due to local changes of λ. In summary, $\psi(\lambda_0, \xi_0)$ represents the total mass transport across the isoline λ_0 and below the isoline ξ_0 (see Figure 4.2). Examples of this kind of stream functions are the hydrothermal in the atmosphere (Kjellsson *et al.*, 2013), and the thermohaline in the ocean (Döös *et al.*, 2012, Groeskamp *et al.*, 2014, Zika *et al.*, 2012).

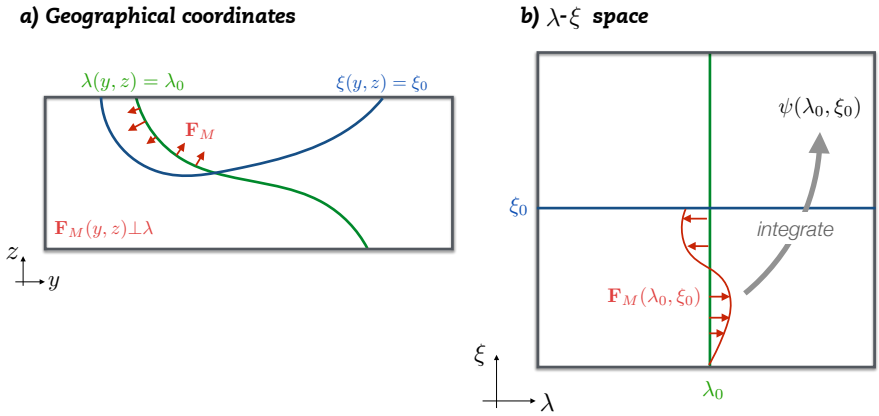

Figure 4.2: Schematic of the computation of $\psi(\lambda_0, \xi_0)$. This is done by projecting F_M in (a) the geographical space onto (b) the tracer $\lambda - \xi$ space. The stream function represents the sum of all the mass fluxes F_M (red arrows) across the isoline $\lambda = \lambda_0$ (green contour) and below the isoline $\xi \leq \xi_0$ (blue contour).

4.3 Helmholtz decomposition

By definition stream functions are constructed over non-divergent fields. However, this requirement is not satisfied, especially in the ocean where precipitation and evaporation for instance act as sources and sinks at the surface. This problem can be solved by applying a Helmholtz decomposition (Arfken & Weber, 1995) on the mass fluxes in the $\lambda - \xi$ space given by their total tendencies. This way we can split the fluxes into a rotational ($\mathbf{F}_M^{RF}$) and a divergent free ($\mathbf{F}_M^{DF}$) components:

$$\mathbf{F}_M(\lambda,\xi) = \left(\Delta\xi\frac{D\lambda}{Dt}, \Delta\lambda\frac{D\xi}{Dt}\right)(\lambda,\xi) = \underbrace{\nabla_{\lambda,\xi}\chi}_{\mathbf{F}_M^{RF}} \quad + \quad \underbrace{\nabla_{\lambda,\xi}\psi \times \hat{e}_3}_{\mathbf{F}_M^{DF}}. \tag{4.5}$$

Here χ is a velocity potential, $\hat{e}_3$ represents the normal vector to the $\lambda - \xi$ plane, and $\nabla_{\lambda,\xi}$ represents the non-dimensional Nabla operator (Groeskamp *et al.*, 2014, Speer, 1993):

$$\nabla_{\lambda,\xi} \equiv \left(\Delta\lambda\frac{\partial}{\partial\lambda}, \Delta\xi\frac{\partial}{\partial\xi}\right), \tag{4.6}$$

with $\Delta\lambda$ and $\Delta\xi$ as the normalisation factors. The normalisation is required due to the different quantities λ and ξ may have.

The stream function $\psi(\lambda,\xi)$ is constructed by selecting the divergent free component $\mathbf{F}_M^{DF}$ and solving a Poisson equation over the curl of the fluxes:

$$\nabla^2_{\lambda,\xi}\psi = -\hat{e}_3 \cdot \left(\nabla_{\lambda,\xi} \times \mathbf{F}_M^{DF}\right) = -\hat{e}_3 \cdot \left(\nabla_{\lambda,\xi} \times \mathbf{F}_M\right). \tag{4.7}$$

4.4 Associated transports

Stream functions can be used to compute different tracer transports. The advantage, compared to other more direct techniques, is the ability to compute transports associated to specific cells in the stream function. This can be useful to quantify the contribution of the different cells and the associated processes.

The tracer transports are computed by integrating the stream function in the tracer space (Ballarotta *et al.*, 2014, Ferrari & Ferreira, 2011),

$$Tr(\lambda) \quad = \quad C_{Tr}\int_{\xi_{min}}^{\xi_{max}} (\xi - \xi_R)\frac{\partial\psi(\lambda,\xi)}{\partial\xi}d\xi, \tag{4.8}$$

where C_{Tr} is a conversion factor that varies depending on the different transports. Table (4.1) shows a list of the most common C_{Tr} choices.

Moreover, ξ_{max} and ξ_{min} are the minimum and maximum values in the ξ-space where $\psi(\lambda,\xi)$ is defined. A reference value of the tracer ξ_R, is usually introduced to minimise the effect of a non-divergent flow. However, this term

Table 4.1: A summary of different C_{Tr} values to compute heat and freshwater transports in the ocean and the atmosphere.

ξ	C_{Tr}	Tracer transport
θ_A	$c_p^{air} = 1004$ J kg^{-1} K^{-1}	Heat transport (atmosphere)
q	$\frac{1}{1000}$ kg g^{-1}	Freshwater transport (atmosphere)
θ_O	$c_p^{water} \approx 3992$ J kg^{-1} K^{-1}	Heat transport (ocean)
S	$\frac{1}{S_R} = \frac{1}{35}$ kg g^{-1}	Freshwater transport (ocean)

is not required if the stream function is computed from a non-divergent field, *i.e.* $\psi(\lambda, \xi_{min}) = \psi(\lambda, \xi_{max}) = 0$. Using this argument, equation (4.8) can be simplified to

$$Tr(\lambda) = -C_{Tr} \int_{\xi_{min}}^{\xi_{max}} \psi(\lambda, \xi) d\xi. \tag{4.9}$$

This transport represents the tracer value across the isoline λ. The meridional tracer transport is obtained by substituting λ by the geographical coordinate y.

5. Stream functions: applied

5.1 Hydrothermohaline stream function

The hydrothermohaline stream function (Döös *et al.*, 2017) is a combination of the atmospheric hydrothermal (Kjellsson *et al.*, 2013) and the oceanic thermohaline (Döös *et al.*, 2012, Zika *et al.*, 2012) stream functions. This stream function is discussed in Paper I and Paper II.

5.1.1 Hydrothermal stream function, $\psi(q, \theta_A)$

The original hydrothermal stream function introduced by Kjellsson *et al.* (2013) describes the atmospheric circulation where latent heat (LH) and dry static energy (DSE) act as coordinates. These coordinates can be translated to specific humidity (q) and potential temperature (θ_A), respectively.

Contrary to the three cells that are observed in a latitude-height space, the hydrothermal stream function is given by a single triangular shaped cell (see Figure 5.1). This cell combines not only the thermodynamic effects of the Hadley and the mid-latitude circulations, but it also includes zonal circulations such as the Walker circulation. In order to describe the main process described by $\psi(q, \theta_A)$ we will consider the outer stream line. Let us start from the edge of the triangle with the largest q – from here the flow continues to larger values of θ_A while q decreases. This side describes the ascension of warm and moist air in the tropical region. As the water vapour condenses and precipitates, LH is transformed into DSE. The second side along the $q = 0$ g kg^{-1} isohume represents the radiative cooling of air masses. Finally, the third side which is bounded by the Clausius-Clapeyron (C-C) relationship describes the warming and moistening of near surface air masses.

Future scenarios show an expansion and weakening of the hydrothermal stream function (see Figure 5.1). The triangular-shaped circulation is maintained and the junction between the moistening and the precipitation branches is shifted to warmer temperatures as a result of the C-C relationship (Kjellsson, 2015).

5.1.2 Thermohaline stream function, $\psi(S, \theta_O)$

Similar to the atmospheric case, the thermohaline stream function (Döös *et al.*, 2012, Zika *et al.*, 2012) describes the ocean circulation using temperature (θ_O)

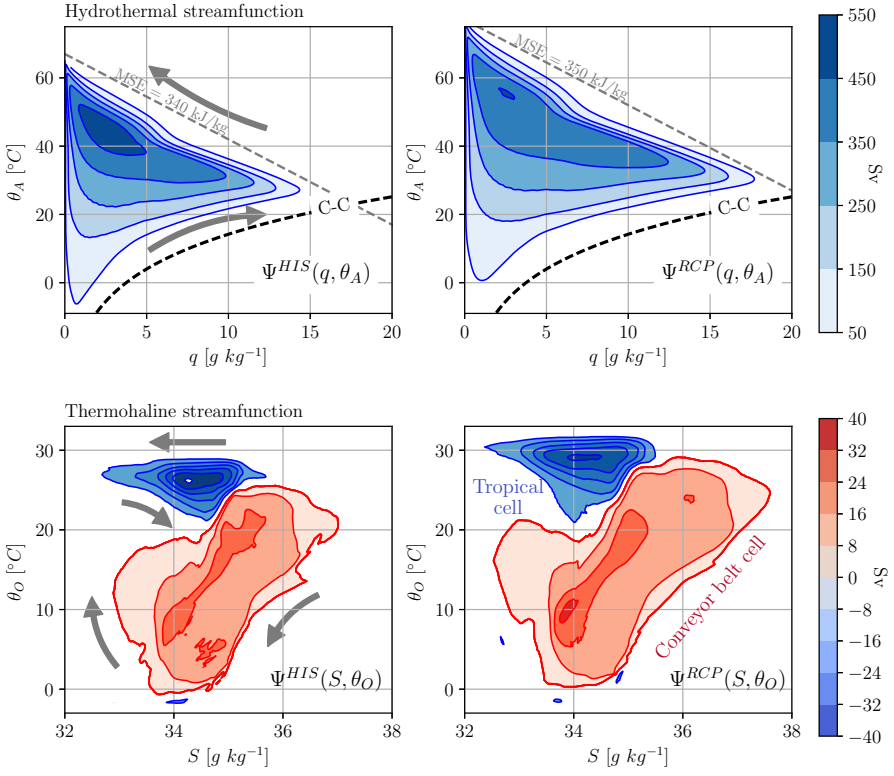

Figure 5.1: Top: hydrothermal stream function for present climate (left) and for the future scenario (right). Bottom: thermohaline stream function for present climate (left) and for the future scenario (right). The grey arrows represent the direction of the streamlines. Figure taken from Paper II.

and salinity (S) as coordinates. This stream function is characterised by two large cells (see Figure 5.1): the tropical cell and the conveyor-belt cell. The tropical cell (blue cell) is the sum of the shallow wind-driven overturning circulations in the three tropical oceans. This tropical cell also includes a contribution from the zonal overturning in particular from the Pacific Ocean. The conveyor-belt cell (red) covers a large span in both temperature and salinity. It describes the inter-basin exchange of water masses. This cell captures from warm and saline waters in the subtropical Atlantic to the fresh and cold waters in the Southern Ocean.

The future projections show a shift towards warmer temperatures of the thermohaline stream function. Large part of the $\psi(S, \theta_O)$ corresponds to water masses near the surface, which explains the rapid adjustment in the future-scenario case. Bottom waters, despite being the most abundant in volume terms, are confined in a small range in the $S - \theta_O$ space. A widening in the S

space is a result of changes in the freshwater forcing. The largest salinification takes place in the Atlantic sector of the thermohaline stream function (Levang & Schmitt, 2015). As a result, the contrast between the Atlantic and the Indo-Pacific basins enhances.

5.2 Latitude–carbon stream function, $\psi(y, C)$

The majority of the studies that use meridional stream functions in latitude-tracer coordinates are based on thermodynamic tracers. In Paper III the thermodynamic tracer is replaced by a biogeochemical tracer such as the dissolved inorganic carbon. The global latitude–C_{tot} stream function is described by five main circulation cells. The cells located between the equator and the mid-latitudes, and with relatively low carbon concentrations represent the big wind-driven subtropical ocean gyres. Another two cells at higher carbon concentrations and spanning through whole ocean basins represent deep and bottom waters. Finally, a small cell is located in the Southern Ocean between 40–60° south, with C_{tot} concentrations of 2100–2300 mmol m^{-3}. This cell can be linked to the activity of the Antarctic Circumpolar Current.

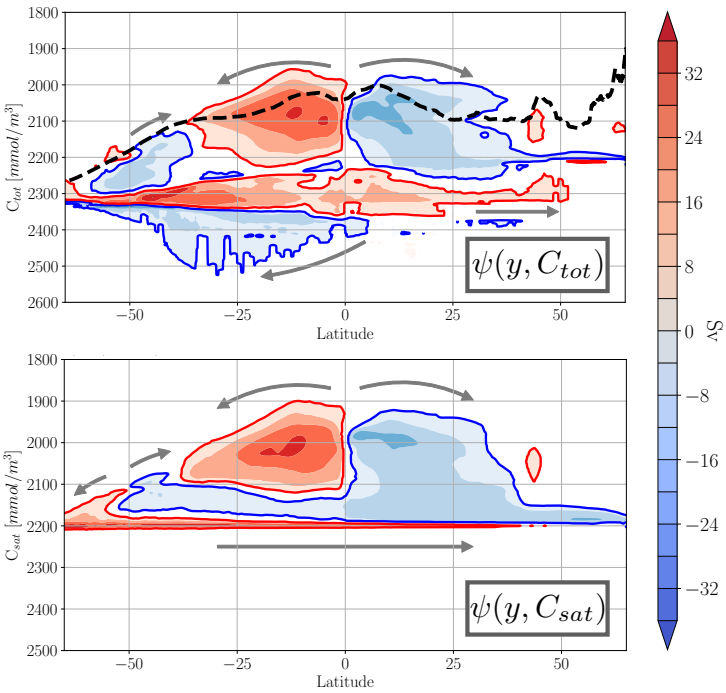

Figure 5.2: Global meridional stream functions for total dissolved inorganic carbon (top) and for the saturation carbon (bottom). The grey arrows represent the direction of the streamlines. For visualisation purposes the tracer coordinate (y-axis) is inversed. Figure adapted from Paper III.

High C_{tot} concentrations are associated with polar waters (due to higher gas solubility in colder water (Raven & Falkowski, 1999, Volk & Hoffert, 2013, Weiss, 1974) and in deep waters due to the biological pump (Broecker, 1983, Volk & Hoffert, 2013)). For visualisation purposes, and in order to have near surface circulation cells above those associated with deep waters, the y-axis has been reversed in Figure 5.2. However, C_{tot} cannot act as pseudo-depth due to the local maxima of carbon concentrations at intermediate depths.

A good biogeochemical tracer that can act as pseudo-depth is the saturation carbon C_{sat}. The associated meridional stream function is very similar to the total carbon one. This stream function is characterised by three cells. The two surface tropical cells and the surface cell in the Southern Ocean can be distinguished. Nevertheless, the Southern Ocean cell is directly connected to the northern tropical cell. Confined to much narrower C_{sat} concentrations of around 2200 mmol m^{-3} the analogy to deep cell can be found.

Saturation carbon is the dominant component in the solubility pump. Therefore, the associated stream function gives a good first approximation of the role of the solubility pump in the ocean. The strong similarity with the density-latitude stream function (shown in *e.g.* Ballarotta *et al.* (2014)), is explained by the strong control that temperature exerts on C_{sat} (Resplandy *et al.*, 2018) and density.

6. The Mediterranean Sea

6.1 The Mediterranean basin

The *Mare Nostrum*[1]- Mediterranean Sea - is the largest enclosed sea on Earth. The basin almost surrounded by land is connected to the Atlantic Ocean through a narrow but deep strait, the Strait of Gibraltar. The Mediterranean Sea can be considered a reversed estuary. Relatively fresh and cold waters from the Atlantic Ocean enter into the basin through the strait. The excess of evaporation over precipitation and river runoff in the majority of the basin drives the formation of denser and more saline waters (see Figure 6.1). This happens in two main regions in particular: the Gulf of Lion where the Western Mediterranean Deep Water (WMDW) is formed, and the Levantine Sea where the Levantine Intermediate Water (LIW) is formed (Bryden & Stommel, 1982, Gascard & Richez, 1985).

The newly formed LIW is the warmest and most saline water mass in the Mediterranean Sea, however, once it reaches the western basin it becomes lighter. Both the WMDW and the LIW merge in the Alboran Sea (south of the Iberian Peninsula) forming the Mediterranean Overflow Water (MOW) (Talley, 1996, Tanhua *et al.*, 2013) which flows back into the Atlantic Ocean (see Figure 6.1).

6.2 The role of the atmosphere

The strength of the flow and the thermodynamic properties of the MOW are strongly linked to atmospheric forcing in the basin. The inflow of Atlantic waters into the Mediterranean Sea is controlled by the wind patterns in the vicinity of the Strait of Gibraltar. An anomaly of the wind pattern both in direction and strength has an impact on the inflow waters, which in turn is responsible for an anomalous outflow. Anomalous outflows through the strait are usually linked to denser and more saline MOW waters (Boutov *et al.*, 2014).

Variations in the freshwater forcing in the basin are mainly driven by changes in the $E - P$ pattern. Two important atmospheric regimes are mainly responsible for this variability (Boutov *et al.*, 2014, Vautard, 1990). These regimes are a consequence of atmospheric pressure fluctuations. The leading

[1] *Mare Nostrum*: latin for "our sea" was the way Romans referred to the Mediterranean Sea.

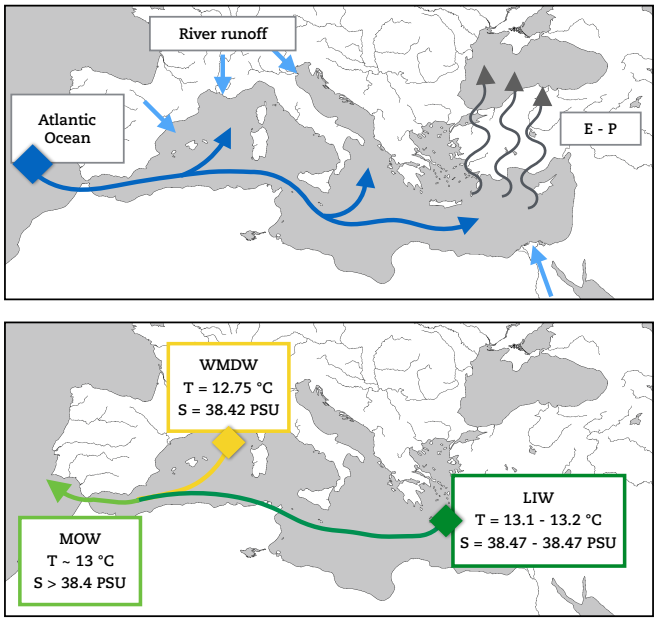

Figure 6.1: Sketch of the inflow (top) and outflow (bottom) pathways. The characteristic temperature and salinity of the main contributors to the Mediterranean Overflow Water are also displayed.

regime is the North Atlantic Oscillation (NAO) which controls the strength of the westerly winds in the North Atlantic. Wetter conditions (increase of P) are observed in the Mediterranean basin under periods of weak westerlies. The second atmospheric regime is related to the Scandinavian Blocking. The strong anticyclone system in Northern Europe associated with this event is responsible for deviating wet air masses southward into the the Mediterranean region (Vautard, 1990).

6.3 The Mediterrean Overflow Water and its role in the Atlantic circulation

After crossing the Strait of Gibraltar, the MOW flows to the Atlantic ocean following the continental slope entraining with the surrounding waters. The high density contrast between the MOW and the Atlantic waters keeps the overflow attached to the continental slope (Baringer & Price, 1997, Price *et al.*, 1993). At an approximate depth of 1000 m the overflow detaches from the slope and spreads westward, filling the entire North Atlantic central basin (see Figure 6.2).

The direct or indirect impact of the MOW to the North Atlantic circulation has been widely discussed. Reid (1979) suggested that an intrusion of the MOW water in the Nordic Seas was possibly affecting the formation of deep water in the region. More recent studies discard Reid's hypothesis suggesting that the warm and saline waters observed in the Nordic Seas were transported by the North Atlantic current (McCartney & Mauritzen, 2001). Lozier & Stewart (2008) brought together both hypotheses, proposing a varying Norwegian–Sea intrusion of the MOW driven by the NAO. The low phase of the NAO linked to a weakening of the westerly winds contributes to a zonal contraction of the subpolar gyre. This would allow the intrusion of the MOW to higher latitudes.

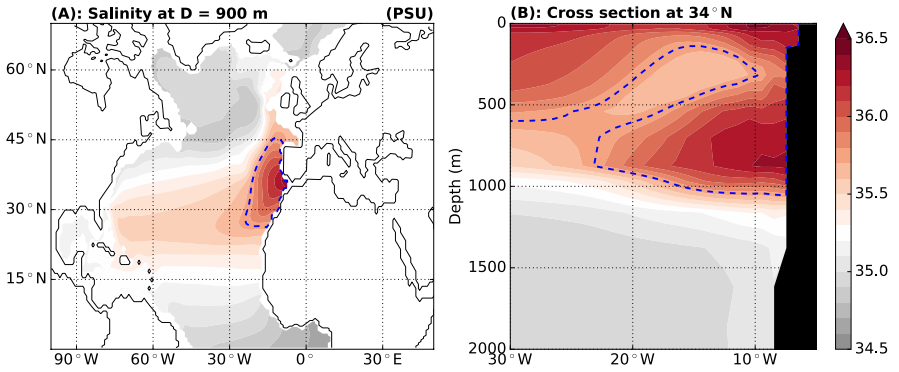

Figure 6.2: (A): The mean salinity field at a depth of 900 metres. The interval between 2 contour lines is 0.1 PSU. (B): Cross section at 34°N showing the saline tongue spreading away from the continental shelf. The core of the MOW is located at around 900 metres depth. The blue dashed contour lines represent the 35.75 PSU isohaline. Figure taken from Paper IV.

In Paper IV the effect of the outflow through the strait of Gibraltar on the Atlantic circulation is discussed. The study focuses on the outward salt transport and its effect on the AMOC. Although the time average of the net salt transport is zero through the strait, a multi-decadal variation is observed. This variability suggests that the Mediterranean basin behaves as a salt reservoir importing and exporting salt from/to the Atlantic Ocean.

7. Final remarks & outlook

Our understanding of the climate system is improving year by year. New sophisticated observational techniques are allowing us to gather more information of different processes that take place in the climate system. Moreover, climate models are becoming more complex by including various new processes, and their resolution is becoming finer. As a result, the amount of climate data is continuously increasing. Hence, so is the need of tools that could help to evaluate and optimise the information gathered.

Among the different set of tools, stream functions defined in different coordinates have been studied in this thesis. Conventional latitude-depth stream functions are commonly used to describe meridional overturning circulations as it is the case for the AMOC (Paper IV). In a more general case, the major features of atmospheric and ocean general circulation can be captured, for example, using stream functions in general thermodynamic coordinates as shown in Paper I and Paper II. Besides, the contribution of the different water masses to the ocean carbon cycle was analysed in Paper III using a stream function in carbon coordinates. This way we are able to understand the impact of different biogeochemical processes which are an important part of the climate system.

However, this is just the tip of the iceberg. With the right choice of coordinates, stream functions become an extremely useful diagnostic tool. Here is a list of possible outlook of the work presented in this thesis:

- All the stream functions computed in this thesis are calculated from model output data. Kjellsson (2015) showed that different models were showing similar hydrothermal stream functions despite having different spatial resolutions. However, this stream function seems to be sensitive to temporal resolution (see Figure 7.1 A). The stream functions presented in Paper I and Paper II are based on 6 hourly model output. With lower temporal resolutions the characteristic single triangular shaped cell of the hydrothermal stream function is lost. Instead, the triangle is split into three cells which fit with the projections of the the Hadley, Ferrel and Polar cells in the $q - \theta_A$ framework (see Figure 7.1 C).

- All the studies presented in this thesis are done from an Eulerian perspective. However, it is possible to compute them using Lagrangian trajectories (*e.g.* Berglund *et al.*, 2017). Using the Lagrangian framework it is possible to distinguish the contribution of different processes which would be complicated to compute in the Eulerian framework (see Figure 7.1 B).

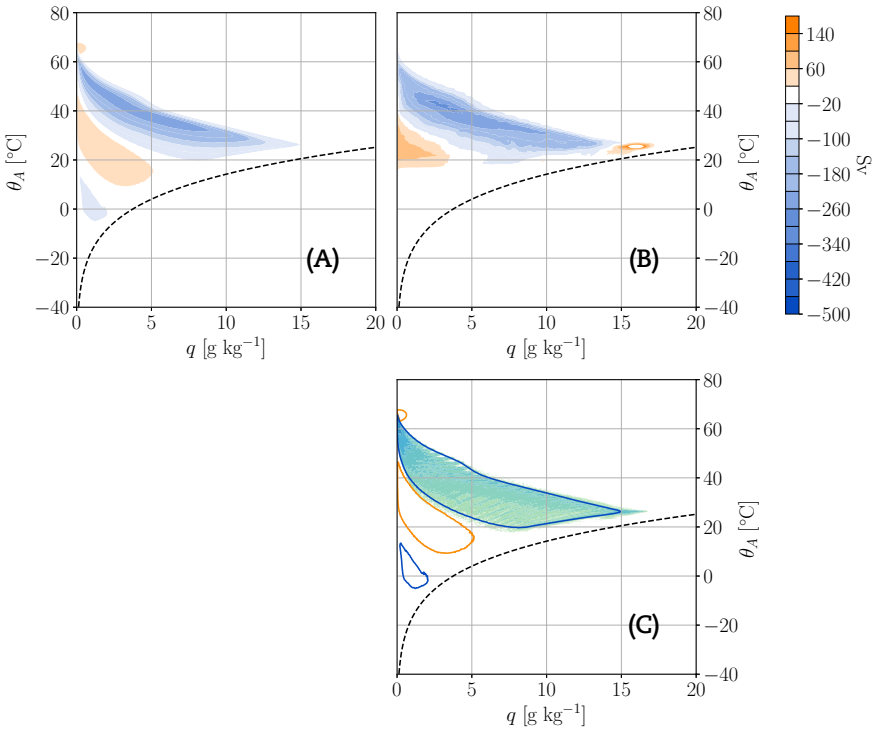

Figure 7.1: (A) The Eulerian hydrothermal stream function for a coarse temporal resolution (monthly mean data). The single cell obtained for finer temporal resolutions is divided into three cells in this case. (B) The hydrothermal stream function computed from Lagrangian trajectories confined inside the tropics. (C) The mass distribution of the air masses of the Hadley cell (fill contours) fits inside one of the cells obtained in the coarse temporal resolution stream function (blue-orange contour lines).

- The study of Paper III can be extended to other relevant biogeochemical tracers beyond the carbon such as oxygen. Ultimately computing a stream function in carbon-oxygen coordinates.

- Finally, the results from Paper IV could be revisited using a Lagrangian framework. This way it could be easier to investigate the role of the outflow waters on the North Atlantic by filtering trajectories according to different selection criteria.

References

Arfken, G.B. & Weber, H.J. (1995). 1 - Vector Analysis. In G.B. Arfken & H.J. Weber, eds., *Mathematical Methods for Physicists (Fourth Edition)*, 1 – 98, Academic Press, Boston, fourth edition edn. 16

Ballarotta, M., Falahat, S., Brodeau, L. & Döös, K. (2014). On the glacial and interglacial thermohaline circulation and the associated transports of heat and freshwater. *Ocean Science*, **10**, 907–921. 16, 22

Baringer, M.O. & Price, J.F. (1997). Mixing and spreading of the Mediterranean outflow. *Journal of Physical Oceanography*, **27**, 1654–1677. 24

Berglund, S., Döös, K. & Nycander, J. (2017). Lagrangian tracing of the water–mass transformations in the Atlantic Ocean. *Tellus A: Dynamic Meteorology and Oceanography*, **69**, 1306311. 27

Bjerknes, J. (1969). Atmospheric teleconnections from the equatorial Pacific. *Monthly weather review*, **97**, 163–172. 4

Blandford, H.F. (1884). On the Connexion of the Himalaya Snowfall with Dry Winds and Seasons of Drought in India. *Proceedings of the Royal Society of London (1854-1905)*, **37**, 3–22. 4

Boutov, D., Peliz, Á., Miranda, P.M., Soares, P.M., Cardoso, R.M., Prieto, L., Ruiz, J. & García-Lafuente, J. (2014). Inter-annual variability and long term predictability of exchanges through the Strait of Gibraltar. *Global and Planetary Change*, **114**, 23–37. 23

Broecker, W.S. (1983). The ocean. *Scientific American*, **249**, 146–161. 22

Broecker, W.S. (1991). The Great Ocean Conveyor. *Oceanography*, **4**. 5

Bryden, H.L. & Stommel, H.M. (1982). Origin of the Mediterranean outflow. *J. Mar. Res*, **40**, 55–71. 23

Caballero, R. & Langen, P.L. (2005). The dynamic range of poleward energy transport in an atmospheric general circulation model. *Geophysical Research Letters*, **32**. 6

Ciais, P., Sabine, C., Bala, G., Bopp, L., Brovkin, V., J. Canadell, A.C., DeFries, R., Galloway, J., Heimann, M., Jones, C., Quéré, C.L., Myneni, R., Piao, S. & Thornton, P. (2014). Chapter 6: Carbon and Other Biogeochemical Cycles. In *Climate Change 2013 - The Physical Science Basis: Working Group I Contribution to the Fifth Assessment Report of the Intergovernmental Panel on Climate Change*, 465–570, Cambridge University Press, Cambridge, United Kingdom, fourth edition edn. 8

Clapeyron, É. (1834). Mémoire sur la puissance motrice de la chaleur. *Journal de l'École polytechnique*, **14**, 153–190. 6

Clausius, R. (1850). Über die bewegende kraft der wärme und die gesetze, welche sich daraus für die wärmelehre selbst ableiten lassen. *Annalen der Physik*, **155**, 368–397. 6

Collins, M., Knutti, R., Arblaster, J., Dufresne, J.L., Fichefet, T., Friedlingstein, P., Gao, X., Gutowski, W., Johns, T., Krinner, G., Shongwe, M., Tebaldi, C., Weaver, A., Wehner, M., Allen, M., Andrews, T., Beyerle, U., Bitz, C., Bony, S. & Booth, B. (2013). *Long-term Climate Change: Projections, Commitments and Irreversibility*, 1029–1136. Intergovernmental Panel on Climate Change, Cambridge University Press, United Kingdom. 7

Couldrey, M.P. (2018). *Mechanisms of ocean carbon cycle variability in the 21st Century*. Ph.D. thesis, University of Southampton. 9

Döös, K. & Nilsson, J. (2011). Analysis of the Meridional Energy Transport by Atmospheric Overturning Circulations. *Journal of the Atmospheric Sciences*, **68**, 1806–1820. 13

Döös, K. & Webb, D.J. (1994). The Deacon cell and the other meridional cells of the Southern Ocean. *Journal of Physical Oceanography*, **24**, 429–442. 13

Döös, K., Nilsson, J., Nycander, J., Brodeau, L. & Ballarotta, M. (2012). The World Ocean Thermohaline Circulation*. *Journal of Physical Oceanography*, **42**, 1445–1460. 13, 15, 19

Döös, K., Kjellsson, J., Zika, J.D., Laliberté, F., Brodeau, L. & Aldama Campino, A. (2017). The Coupled Ocean - Atmosphere Hydrothermohaline Circulation. *Journal of Climate*, **30**, 631–647. 7, 11, 19

Durack, P.J., Wijffels, S.E. & Matear, R.J. (2012). Ocean Salinities Reveal Strong Global Water Cycle Intensification During 1950 to 2000. *Science*, **336**, 455–458. 7

Eggleston, S. & Galbraith, E.D. (2018). The devil's in the disequilibrium: Multi-component analysis of dissolved carbon and oxygen changes under a broad range of forcings in a general circulation model. *Biogeosciences*, **15**, 3761–3777. 9

Eliot, J. (1895). Droughts and famines in India. *Report of the International Meteorological Congress, held at Chicago, Ill., August 21-24, 1893*, 444–459. 4

Ellis, H. & Hales, S. (1751). A Letter to the Rev. Dr. Hales, F. R. S. from Captain Henry Ellis, F. R. S. Dated Jan. 7, 1750-51, at Cape Monte Africa, Ship Earl of Hallifax. *Philosophical Transactions of the Royal Society of London Series I*, **47**, 211–214. 1

Ferrari, R. & Ferreira, D. (2011). What processes drive the ocean heat transport? *Ocean Modelling*, **38**, 171–186. 16

Ferrel, W. (1856). An essay on the winds and currents of the ocean. *Nashville J. Med. & Surg.*, **11**, 287–301. 3

Ferrel, W. (1859). The influence of the Earth's rotation upon the relative motion of bodies near its surface. *Astronomical Journal*, **5**, 97–100. 3

Frierson, D.M. & Hwang, Y.T. (2012). Extratropical influence on ITCZ shifts in slab ocean simulations of global warming. *Journal of Climate*, **25**, 720–733. 6

Gascard, J.C. & Richez, C. (1985). Water masses and circulation in the western Alboran Sea and in the Straits of Gibraltar. *Progress in Oceanography*, **15**, 157–216. 23

Gent, P.R. (2018). A commentary on the Atlantic meridional overturning circulation stability in climate models. *Ocean Modelling*, **122**, 57 – 66. 7

Groeskamp, S., Zika, J.D., McDougall, T.J., Sloyan, B.M. & Laliberté, F. (2014). The Representation of Ocean Circulation and Variability in Thermodynamic Coordinates. *Journal of Physical Oceanography*, **44**, 1735–1750. 15, 16

Hadley, G. (1735). Concerning the cause of the general trade-winds. *Philosophical Transactions of the Royal Society*, **39**, 58–62. 3

Halley, E. (1686). An Historical Account of the Trade Winds, and Monsoons, Observable in the Seas between and Near the Tropicks, with an Attempt to Assign the Phisical Cause of the Said Winds. *Philosophical Transactions of the Royal Society*, **16**, 153–168. 3

Hannachi, A., Jolliffe, I. & Stephenson, D. (2007). Empirical orthogonal functions and related techniques in atmospheric science: A review. *International Journal of Climatology: A Journal of the Royal Meteorological Society*, **27**, 1119–1152. 2

Hazeleger, W., Severijns, C., Semmler, T., Ştefanescu, S., Yang, S., Wang, X., Wyser, K., Dutra, E., Baldasano, J.M., Bintanja, R., Bougeault, P., Caballero, R., Ekman, A.M.L., Christensen, J.H., Van Den Hurk, B., Jimenez, P., Jones, C., Kållberg, P., Koenigk, T., McGrath, R., Miranda, P., Van Noije, T., Palmer, T., Parodi, J.A., Schmith, T., Selten, F., Storelvmo, T., Sterl, A., Tapamo, H., Vancoppenolle, M., Viterbo, P. & Willén, U. (2010). EC-Earth: A seamless Earth-system prediction approach in action. *Bulletin of the American Meteorological Society*, **91**, 1357–1363. 11

Hazeleger, W., Wang, X., Severijns, C., Stefanescu, S., Bintanja, R., Sterl, A., Wyser, K., Semmler, T., Yang, S., van den Hurk, B., van Noije, T., van der Linden, E. & van der Wiel, K. (2012). EC-Earth V2.2: Description and validation of a new seamless earth system prediction model. *Climate Dynamics*, **39**, 2611–2629. 11

Held, I.M. & Soden, B.J. (2000). Water vapor feedback and global warming. *Annual review of energy and the environment*, **25**, 441–475. 7

Held, I.M. & Soden, B.J. (2006). Robust responses of the hydrological cycle to global warming. *Journal of climate*, **19**, 5686–5699. 7

Hwang, Y.T. & Frierson, D.M. (2010). Increasing atmospheric poleward energy transport with global warming. *Geophysical Research Letters*, **37**. 6

IPCC (2013). *Summary for Policymakers*. Climate Change 2013: The Physical Science Basis. Contribution of Working Group I to the Fifth Assessment Report of the Intergovernmental Panel on Climate Change, Cambridge University Press, Cambridge, United Kingdom and New York, NY, USA. 6

Ito, T. & Follows, M.J. (2005). Preformed phosphate, soft tissue pump and atmospheric CO_2. *Journal of Marine Research*, **63**, 813–839. 9

Kjellsson, J. (2015). Weakening of the global atmospheric circulation with global warming. *Climate Dynamics*, **45**, 975–988. 19, 27

Kjellsson, J., Döös, K., Laliberté, F.B. & Zika, J.D. (2013). The Atmospheric General Circulation in Thermodynamical Coordinates. *Journal of the Atmospheric Sciences*, **71**, 916–928. 13, 15, 19

Kuhlbrodt, T., Griesel, A., Montoya, M., Levermann, A., Hofmann, M. & Rahmstorf, S. (2007). On the driving processes of the Atlantic meridional overturning circulation. *Reviews of Geophysics*, **45**. 5, 6

Laliberté, F., Zika, J., Mudryk, L., Kushner, P., Kjellsson, J. & Döös, K. (2015). Constrained work output of the moist atmospheric heat engine in a warming climate. *Science*, **347**, 540–543. 6

Lauderdale, J.M., Garabato, A.C.N., Oliver, K.I.C., Follows, M.J. & Williams, R.G. (2013). Wind-driven changes in Southern Ocean residual circulation, ocean carbon reservoirs and atmospheric CO_2. *Climate dynamics*, **41**, 2145–2164. 9

Levang, S.J. & Schmitt, R.W. (2015). Centennial Changes of the Global Water Cycle in CMIP5 Models. *Journal of Climate*, **28**, 6489–6502. 7, 21

Lozier, M.S. & Stewart, N.M. (2008). On the temporally varying northward penetration of Mediterranean Overflow Water and eastward penetration of Labrador Sea Water. *Journal of Physical Oceanography*, **38**, 2097–2103. 25

Madec, G. *et al.* (2015). NEMO ocean engine, Note du Pole de modélisation, Institut Pierre-Simon Laplace (IPSL), France, No 27. 11

McCartney, M.S. & Mauritzen, C. (2001). On the origin of the warm inflow to the Nordic Seas. *Progress in Oceanography*, **51**, 125–214. 25

Neelin, J.D., Battisti, D.S., Hirst, A.C., Jin, F.F., Wakata, Y., Yamagata, T. & Zebiak, S.E. (1998). Enso theory. *Journal of Geophysical Research: Oceans*, **103**, 14261–14290. 4

Nycander, J., Nilsson, J., Döös, K. & Broström, G. (2007). Thermodynamic Analysis of Ocean Circulation. *Journal of Physical Oceanography*, **37**, 2038–2052. 13

Ödalen, M., Nycander, J., Oliver, K.I.C., Brodeau, L. & Ridgwell, A. (2018). The influence of the ocean circulation state on ocean carbon storage and CO_2 drawdown potential in an Earth system model. *Biogeosciences*, **15**, 1367–1393. 9

Pauluis, O., Czaja, A. & Korty, R. (2010). The global atmospheric circulation in moist isentropic coordinates. *Journal of Climate*, **23**, 3077–3093. 13

Pauluis, O.M. & Mrowiec, A.a. (2013). Isentropic Analysis of Convective Motions. *Journal of the Atmospheric Sciences*, **70**, 3673–3688. 13

Pauthenet, E., Roquet, F., Madec, G., Sallé, J.B. & Nerini, D. (2019). The thermohaline modes of the global ocean. *Journal of Physical Oceanography*, **0**, null. 2

Peixoto, J.P. & Oort, A.H. (1992). *Physics of climate*. New York, NY (United States); American Institute of Physics. 3

Philander, S.G.H. (1983). El Niño Southern Oscillation phenomena. *Nature*, **302**, 295. 4

Price, J.F., Baringer, M.O., Lueck, R.G., Johnson, G.C., Ambar, I., Parrilla, G., Cantos, A., Kennelly, M.A. & Sanford, T.B. (1993). Mediterranean outflow mixing and dynamics. *Science*, **259**, 1277–1282. 24

Rasmusson, E.M. & Carpenter, T.H. (1982). Variations in tropical sea surface temperature and surface wind fields associated with the Southern Oscillation/El Niño. *Monthly Weather Review*, **110**, 354–384. 4

Raven, J. & Falkowski, P. (1999). Oceanic sinks for atmospheric CO_2. *Plant, Cell & Environment*, **22**, 741–755. 22

Redfield, A.C. (1934). On the proportions of organic derivatives in sea water and their relation to the composition of plankton. *James Johnstone memorial volume*, 176–192. 12

Reid, J.L. (1979). On the contribution of the Mediterranean Sea outflow to the Norwegian-Greenland Sea. *Deep Sea Research Part A. Oceanographic Research Papers*, **26**, 1199–1223. 25

Resplandy, L., Keeling, R.F., Rödenbeck, C., Stephens, B.B., Khatiwala, S., Rodgers, K.B., Long, M.C., Bopp, L. & Tans, P.P. (2018). Revision of global carbon fluxes based on a reassessment of oceanic and riverine carbon transport. *Nature Geoscience*, **11**, 504–509. 22

Richardson, P.L. (2008). On the history of meridional overturning circulation schematic diagrams. *Progress in Oceanography*, **76**, 466–486. 5

Sarmiento, J.L. & Gruber, N. (2006). *Ocean Biogeochemical Dynamics*. Princeton University Press. 9

Schneider, T., O'Gorman, P.A. & Levine, X.J. (2010). Water vapor and the dynamics of climate changes. *Reviews of Geophysics*, **48**. 6

Speer, K.G. (1993). Conversion among North Atlantic surface water types. *Tellus A*, **45**, 72–79. 16

Talley, L.D. (1996). North Atlantic circulation and variability, reviewed for the CNLS conference. *Physica D: Nonlinear Phenomena*, **98**, 625–646. 23

Talley, L.D. (2013). Closure of the Global Overturning Circulation Through the Indian, Pacific, and Southern Oceans: Schematics and Transports. *Oceanography*, **26**. 5, 6

Tanhua, T., Hainbucher, D., Schroeder, K., Cardin, V., Álvarez, M. & Civitarese, G. (2013). The Mediterranean Sea system: a review and an introduction to the special issue. *Ocean Science*, **9**, 789–803. 23

Thomson, B.v.G. (1797). The complete works of Count Rumdorf. *(published in 1870 by the American Academy of Sciences, Boston)*, 329–330. 1, 4

Thomson, J. (1857). On the grand currents of atmospheric circulation. *Transactions of the sections*, 38–39. 3

Vautard, R. (1990). Multiple weather regimes over the North Atlantic: Analysis of precursors and successors. *Monthly weather review*, **118**, 2056–2081. 23, 24

Vecchi, G.A. & Soden, B.J. (2007). Global warming and the weakening of the tropical circulation. *Journal of Climate*, **20**, 4316–4340. 6

Vecchi, G.A., Soden, B.J., Wittenberg, A.T., Held, I.M., Leetmaa, A. & Harrison, M.J. (2006). Weakening of tropical Pacific atmospheric circulation due to anthropogenic forcing. *Nature*, **441**, 73. 6

Volk, T. & Hoffert, M.I. (1985). Ocean Carbon Pumps: Analysis of Relative Strengths and Efficiencies in Ocean–Driven Atmospheric CO_2 Changes. In E.T. Sundquist & W.S. Broecker, eds., *The Carbon Cycle and Atmospheric CO_2: Natural Variations Archean to Present*, 99–110, American Geophysical Union, Washington D.C. 8, 9

Volk, T. & Hoffert, M.I. (2013). *Ocean Carbon Pumps: Analysis of Relative Strengths and Efficiencies in Ocean-Driven Atmospheric CO_2 Changes*, 99–110. American Geophysical Union (AGU). 8, 9, 22

Walker, G.T. (1924). Correlations in seasonal variations of weather. I. A further study of world weather. *Mem. Indian Meteorol. Dep.*, **24**, 275–332. 4

Wallace, J.M. & Hobbs, P.V. (2006). *Atmospheric science: An introductory survey*. International geophysics series, Elsevier, 2nd edn. 6

Weaver, A.J., Sedláček, J., Eby, M., Alexander, K., Crespin, E., Fichefet, T., Philippon-Berthier, G., Joos, F., Kawamiya, M., Matsumoto, K. *et al.* (2012). Stability of the Atlantic meridional overturning circulation: A model intercomparison. *Geophysical Research Letters*, **39**. 6

Weiss, R. (1974). Carbon dioxide in water and seawater: the solubility of a non-ideal gas. *Marine chemistry*, **2**, 203–215. 22

Williams, R.G. & Follows, M.J. (2011). *Ocean Dynamics and the Carbon Cycle: Principles and mechanisms*. Cambridge University Press, Cambridge. 9

Yool, A., Popova, E.E. & Anderson, T.R. (2013). MEDUSA-2.0: An intermediate complexity biogeochemical model of the marine carbon cycle for climate change and ocean acidification studies. *Geoscientific Model Development*, **6**, 1767–1811. 12

Yool, A., Popova, E.E. & Coward, A.C. (2015). Future change in ocean productivity : Is the Arctic the new Atlantic? *Journal of Geophysical Research Oceans*, **120**, 7771–7790. 12

Zickfeld, K., Eby, M. & Weaver, A.J. (2008). Carbon-cycle feedbacks of changes in the Atlantic meridional overturning circulation under future atmospheric CO_2. *Global Biogeochemical Cycles*, **22**. 6

Zika, J.D., England, M.H. & Sijp, W.P. (2012). The Ocean Circulation in Thermohaline Coordinates. *Journal of Physical Oceanography*, **42**, 708–724. 13, 15, 19

Zika, J.D., Skliris, N., Nurser, a.J.G., Josey, S.a., Mudryk, L., Laliberté, F. & Marsh, R. (2015). Maintenance and broadening of the ocean's salinity distribution by the water cycle. *Journal of Climate*, 9550–9560. 7

Zika, J.D., Skliris, N., Blaker, A.T., Marsh, R., Nurser, A.G. & Josey, S.A. (2018). Improved estimates of water cycle change from ocean salinity: the key role of ocean warming. *Environmental Research Letters*, **13**, 074036. 7

Acknowledgements

This thesis wouldn't have been possible without the support and guidance of my two supervisors. My deepest gratitude to Kristofer Döös for his patience, for all the scientific discussions and not so scientific discussions, and for all support shown during the last fiver years. Peter Lundberg, thank you for sharing all your knowledge and giving very constructive comments to improve my work. I would also like to thank Laurent Brodeau, who was my co-supervisor for a short period of time, for all his technical support, providing data and for making me hesitate whether I was a graphical designer or a scientist. I would also like to thank my committee members Gunilla Svensson and Frida Bender for making sure I was on track during my PhD. Special thank you to Fabien Roquet, for jumping in as a committee member when needed, and for all his support and advice. Finally, I would like to acknowledge the whole oceanography group at MISU and all the co-authors, in particular Joakim Kjellsson for all the great scientific discussions and constructive comments, and Sjoerd Groeskamp for his warm welcome during my time in Australia.

I would like to give a special thank you to a wonderful group of people who have been part of this adventure since the first day. Xiang-Yu, thank you for forcing me to do some exercise and for all the great excursions, dinners and trips we have shared. Maartje, although you started a bit later you are a true member of our generation. Thank you for being there when I needed and for all the dinners, BBQs, excursions, ... I hope you don't forget your Spanish lessons. Lena, thank you for all the baking, swimming evenings and dinners. Waheed, I have no idea how I will survive without your cooking from now on. It has been a great honour knowing you and sharing the PhD experience with you. Finally but not least, I would like to thank Etienne for being such a good friend during the past five years. Thank you for all the lunches, afterworks, dinners, conference trips, etc. and for always being there to listen and help when I needed.

I think I may have broken the record of office moves in the history of MISU (6 times in 5 years), but thanks to that I have had the privilege of sharing the office with great people. I would like to thank Abubakr for his warm welcoming and support during my first year as PhD student, and for all the great discussions we had. Lina for keeping my Swedish updated and making sure I would not forget it. Koen for providing shelter when the roof of the office collapsed, and for all the dinners, game evenings and trips in these last five years. Qin for all the good science discussions and for making sure that my

name got properly written in Chinese. Special thank you to Henrik and Filippa for "adopting" me in your office while you were finishing your PhDs. I hope I wasn't a burden to you. Thank you Henrik (PyNinja) for all the programming and Python tips that have made my life much easier. Filippa, thank you for the Mac screen that helped me procastinate making new figures and for all the plants in the office. It was great to work together on the carbon paper. Finally but not least, a very special thank you to my current office mates and fellow minions: Dipanjan and Sara (beta), without you I'm not sure if I would have completed this PhD. Dipanjan, thank you for all the discussions and for all the good times. Don't think I have forgotten it, but one way or another you will be part of a Luciatåg at some point. Sara, thank you for keeping me within my sanity limits and putting up with my short moments of panic. It has been a honour being your officemate all these years.

I wouldn't have survived to this PhD without the help of my mentor, Malin. Thank you for all the tips, advice, and help. I am very happy that we have worked together in the carbon paper (thank you for introducing me into the biogeochemistry world) and that we are finishing at the same time. I keep your word about a trip to Norrland. Special thank you to Sara (alpha) for dealing with my math problems and for making sure that I wouldn't miss the new season of "Bikings". Tongmei, thank you for all the dinners at your place, for providing proper tea and for always being there to help. I would also like to thank Friederike H. for helping me through all the final steps of this thesis. Finally I would like to acknowledge MISU's TA staff, postdocs, and the rest of the PhD fellows: Ines, Erik, Evelien, Sebastian, Roman, Jakob, Cheng, Martin, Alejandro, Alejandro U., Sonja, Martin, Marin, Eva, Charlotta, Cian, Quentin, Clara, Nav, Srinath, Anna.

There is also life outside MISU. First of all I would like to thank Ulf for not just being the best landlord one could ask, but for being a very good friend and a great ambassador of Sweden. Thank you for all the great moments, chats, dinners and for making me feel like home everyday. I am also very grateful to Åsa, Cecilia, Johan, Aitor V. and Laura for making these years more bearable. Special thank you to Friederike P., Benedikt, Jasone (you still owe me a visit), Mikel, Julen, Jon, Alba, Irati and Javi for all the support given from the distance. My deepest gratitude to a very special person Karolina, thank you for all your strength and dealing with all my stress times. Thank you for always being there, for your kindness and support.

Finally, I wouldn't have survived all this years away from home without the support of my family. My deepest gratitude goes to all of them, especially to my aunt Ainara, my sister Amaia, and my parents Bego and Josu. *Eskerrik asko bihotz-bithotzez.*